

A Surrogate Reduced Order Free Vibration Model of Linear and Non-Linear Beams using Modified Modal Coefficients and HOSVD Approaches

Mohammad Kazem Moayyedi*

Department of Mechanical Engineering,
University of Qom, Iran

E-mail: mk.moayyedi@qom.ac.ir

*Corresponding author

Received: 5 June 2018, Revised: 27 September 2018, Accepted: 17 December 2018

Abstract: In the present work, two low-dimensional models are presented and used for vibration simulation of the linear and non-linear beam models. These models help to compute the dynamical responses of the beam with fast computation speed and under the effects of different conditions. Also the obtained results can be used in the conceptual and detailed design stages of an engineering system overall design. First, a finite element analysis based on Euler-Bernoulli beam elements with two primary variables (deflection and slope) at each node is used to find static and dynamic responses of the considered linear and non-linear beams. Responses to three different static load cases are obtained and applying them as initial conditions, the time responses of the beam are calculated by the Newmark's time approximation scheme. A low-dimensional POD model which was extracted from the ensemble under the effect of an arbitrary loading is reconstructed. To apply the model to simulate the response of beam under the effect of other loads, POD modal coefficients are updated due to change of initial condition. This modification is performed based on the recalculation of the eigenvalues due to a new initial condition. Also, another low-dimensional model is constructed which is developed based on an ensemble under the effect of several parameters. To apply the model to simulate the response of the beam under the effect of other loads and variations of beam thickness, POD-HOSVD modal coefficients are updated due to the change of desired parameters. The results obtained from the low-dimensional model are showing good agreement to the benchmark data and proving high level accuracy of the model.

Keywords: Free Vibration, High Order Singular Value Decomposition, Low-Dimensional Model, Proper Orthogonal Decomposition, Structural Dynamics

Reference: Moayyedi, M. K., "A Surrogate Reduced Order Free Vibration Model of Linear and Non-Linear Beams Using Modified Modal Coefficients and HOSVD Approaches", *Int J of Advanced Design and Manufacturing Technology*, Vol. 11/No. 4, 2018, pp. 61–71.

Biographical notes: **Mohammad Kazem Moayyedi** received his PhD from Sharif University of Technology in 2009. He is currently Assistant Professor at the Department of Mechanical Engineering, University of Qom, Iran. His current research interests include Reduced Order Modeling of Dynamical System and Computational Modeling of Fluid-Solid Interaction.

1 INTRODUCTION

Proper orthogonal decomposition (POD) is a method for extracting the dominant structures of a dynamical system by modal decomposition of an ensemble. This assembly contains system responses with respect to some parameters such as time. A significant property of the POD method is its optimality for identification of the most energetic structures of a problem. Although POD has been regularly applied to non-linear problems, it is essential to underline that it is a linear technique and that is optimal only with respect to other linear representations. Reduced order models help scientist and engineers to test and examine their new ideas and experiments in a low cost computational environment. POD method is one of the most interesting approaches for construction of the engineering problems' reduced order models. The Low dimensional POD models have prepared new foundations in computational simulations of the engineering problems. In this research, POD method has been used for both low-order descriptions of the linear and non-linear beam vibration.

A historical review of POD was demonstrated in reference [1]. This method was firstly used by Karhunen & Loeve for statistical data analysis [2]. In 1967, Lumley used this method for extracting large-scale structures of turbulent flows [3]. Then, due to the limitations of computer hardware and that of numerical methods, its usage was stopped. The snapshots method proposed by Sirovich, demonstrated that the POD method could be a useful tool in developing the reduced order models for complex dynamical systems. The required data for these models are obtained through experimental tests or direct numerical simulation [4]. Due to the POD ability in extracting the high-level energy modes, this method can be used for the fluid and structure interactions, the structures response and the flow control problems [5], [6]. Feeny and Kappagantu showed the possibility of using POD as the model analysis supplement when response measurements are available [7].

Han used an approach which was based on linking POD and structural normal modes to extract the structures' mode shapes without measuring a series of frequency response functions [8]. Kereschen et al. studied the application of POD approach for physical interpretation of structural dynamics problems [9]. Han et al. investigated the POD method application for the mode shapes extraction of free vibration of a beam using experimental response data. They showed that the degree of deviation of the other extracted proper orthogonal modes from the true normal modes of the structure depends on the spatial resolution [10]. Amabili et al. studied the nonlinear response of perfect and imperfect, simply supported circular cylindrical shells completely contain an incompressible and inviscid fluid

at rest. The reduced-order models (ROM) are reconstructed using Galerkin POD method. They used different proper orthogonal modes which have been computed from time series at different excitation frequencies [11]. Lieu and Farhat used POD method to produce accurate ROMs for the aeroelastic analysis of complete aircraft configurations at fixed flight conditions. They applied a new ROM adaptation scheme and evaluated for varying Mach number and angle of attack. Good correlations are observed in their results [12]. Gonçalves et al. used Galerkin POD low-Dimensional model for Non-linear vibration analysis of cylindrical thin shells. The outcome model has been applied for analysis of non-linear vibrations and dynamic stability of a circular cylindrical shell subjected to dynamic axial loads [13].

Development of ROM for the dynamics of geometrically exact planar rods based on the projection of the nonlinear equations of motion onto a subspace spanned by a set of proper orthogonal modes is studied by Georgiou. He reported that the POD-based reduced order system provides a potentially valuable tool to characterize the spatio-temporal complexity of the dynamics in order to elucidate connections between proper orthogonal modes and nonlinear normal modes of vibration [14]. Allison used the proper orthogonal decomposition of measured response data combined with the linear system theory to construct a model for predicting the response of an arbitrary linear or nonlinear system without any knowledge of the equations of motion [15].

Gonçalves et al. investigated the development of the ROM for the nonlinear vibration analysis of cylindrical shells based on a perturbation procedure and proper orthogonal decomposition. They used this model for analysis of the nonlinear vibrations and dynamic stability of a circular cylindrical shell subjected to static and dynamic loads [16]. Paulo et al. studied the reduced order model construction for the nonlinear dynamic analysis of shells. They have been applied a perturbation analyses together with the Galerkin method which can be used to derive precise low order models for plates and shells, by capturing the influence of the modal couplings and interactions [17]. Speet studied about the reduced order frameworks for structural models using a manifold interpolation method. His methodology interpolated between the pre-calculated reduced order models and their corresponding reduced order basis [18].

Ilbeigi developed a parametric form of reduced order models for simulation of complex non-linear dynamical systems under the effects of different parameters and signals [19]. A non-intrusive reduced basis method was used for parameterized nonlinear structural analysis undergoing large deformations by Guo and Hesthaven. In this method, principal mode shapes are calculated by the proper orthogonal decomposition (POD), and the

Gaussian process regression is used to approximate the projection coefficients [20].

Finally, in this research, a reduced order model is developed using two approaches. In the first method, the model is constructed based on data which is obtained for specified conditions and in the second, a low-order framework using the HOSVD method is developed. Therefore, the first model can be used for any set of initial conditions to simulate the dynamical behavior of linear and non-linear beam models. Also, the second model, which is constructed using a tensor- based data set, can be used to simulate the response of the linear and non-linear beams under the effects of important related parameters.

In the sequel, the principal concepts of the POD are presented. In the next section, the mathematical formulation and numerical algorithm of finite element model are presented. Then, the low order proper orthogonal decomposition and HOSVD models are discussed. The order reduction criterion and our results are discussed in the next sections.

2 PROPER ORTHOGONAL DECOMPOSITION

The POD Reduced-order modelling begins by finding the empirical Eigen functions using the Karhunen-Loève decomposition. Then the flow variables are approximated using expansions of these eigenmodes. The governing equations are projected into the eigenfunctions space to obtain the sets of equations for the coefficients of the expansions that can be solved to predict the behavior of the flow variables in space and time. POD is remarkable in that the selection of bases functions is not just appropriate, but optimal which is described further in the analysis section. The POD was introduced to the turbulence community by Lumley in 1967. Before that, it was already known in statistics as the Karhunen-Loève expansion. Lumley proposed that a coherent structure can be defined with functions of the spatial variables that have maximum energy content. That is, coherent structures are linear combinations of Φ 's, which maximizes the following expression [2]:

$$\max \frac{\langle (\Phi, \mathbf{u})^2 \rangle}{\Phi, \Phi}, \quad (1)$$

Where, (Φ, \mathbf{u}) is the inner product of the basis vector Φ with the field, \mathbf{u} . Note $\langle \cdot \rangle$ is the time-averaging operation. It can be shown that the POD basis vectors are eigenfunctions of the Kernel \mathbf{K} given by:

$$\mathbf{K} = \langle \mathbf{u}, \mathbf{u}' \rangle, \quad (2)$$

Where, \mathbf{u}' denotes the Hermitian of \mathbf{u} . This equation is converted to the Fredholm's second kind integral equation and its discretization leads to an eigenvalue problem. In this work, the SVD method has been used to solve this eigenvalue problem [5].

3 FINITE ELEMENT MODELLING

A fourth-order differential equation known as the Euler-Bernoulli beam equation is applied in FE modelling:

$$\frac{\partial^2}{\partial x^2} \left(EI \frac{\partial^2 w}{\partial x^2} \right) - \rho I \frac{\partial^4 w}{\partial x^2 \partial t^2} + \rho A \frac{\partial^2 w}{\partial t^2} = q, \quad (3)$$

Where $w(x,t)$ is the transverse deflection along the beam, E is the Young's modulus, I is the moment of inertia of the beam section, A is the cross-section area and $q = q(x,t)$ is the distributed load along the beam [21]. The weak form of the integral equation over a typical element (x_e to x_{e+1}) is then as follows (1):

$$\int_{x_e}^{x_{e+1}} \left[\frac{\partial^2 v}{\partial x^2} \left(EI \frac{\partial^2 w}{\partial x^2} \right) + \rho I \frac{\partial v}{\partial x} \frac{\partial^3 w}{\partial x \partial t^2} + \rho A v \frac{\partial^2 w}{\partial t^2} - vq \right] dx + v \left[\frac{\partial}{\partial x} \left(EI \frac{\partial^2 w}{\partial x^2} \right) - EI \frac{\partial v}{\partial x} \frac{\partial^2 w}{\partial x^2} - \rho I \frac{\partial^2 w}{\partial t^2 \partial x} \right], \quad (4)$$

Where v is some weight function and according to Galerkin's method and is chosen equal to the interpolation function ψ_j , used in approximation:

$$w^e(x,t) = \sum_{j=1}^4 u_j^e(t) \psi_j^e(x), \quad (5)$$

Where u_j^e are the time-dependent nodal variables of the beam element which are defined as: $u_1^e = w_e$, deflection at the beginning node, $u_2^e = \theta_e$, the slope at the beginning node, $u_3^e = w_{e+1}$, the deflection at the end node, and $u_4^e = \theta_{e+1}$, the slope at the end node. The functions ψ_j^e , interpolating w as well as dw/dZ , are defined in the form of Hermite cubic functions as follows:

$$\psi_j^e(x) = \varphi_j^e(\xi), \quad \xi = \frac{x - x_e}{L_e}, \quad j = 1, \dots, 4 \quad (6)$$

$$\begin{aligned}\varphi_1^e(\xi) &= 1 - 3\xi^2 + 2\xi^3, \\ \varphi_2^e(\xi) &= -L_e\xi^2(1 - \xi^2), \\ \varphi_3^e(\xi) &= 3\xi^2 - 2\xi^3, \\ \varphi_4^e(\xi) &= -L_e\xi(\xi^2 - \xi),\end{aligned}$$

Where, L_e is the element length. The element ODE is then derived by applying approximation (5) into the weak formulation (4) which in the absence of structural damping yields the matrix equation:

$$M^e \ddot{u}^e + C^e \dot{u}^e + K^e u^e = F^e, \quad (7)$$

Where:

$$\begin{aligned}M_{ij}^e &= \int_{x_e}^{x_{e+1}} \left(\rho A \psi_i^e \psi_j^e + \rho I \frac{d\psi_i^e}{dx} \frac{d\psi_j^e}{dx} \right) dx, \\ K_{ij}^e &= \int_{x_e}^{x_{e+1}} EI \frac{d^2\psi_i^e}{dx^2} \frac{d^2\psi_j^e}{dx^2} dx, \\ F_i^e &= \int_{x_e}^{x_{e+1}} \psi_i^e q dx + Q_i^e, \\ Q_1^e &= \left[\frac{\partial}{\partial x (EI \frac{\partial^2 w}{\partial x^2})} - \rho I \frac{\partial^3 w}{\partial^2 t \partial x} \right], \\ Q_2^e &= \left[EI \frac{\partial^2 w}{\partial x^2} \right], \\ Q_3^e &= \left[\frac{\partial}{\partial x (EI \frac{\partial^2 w}{\partial x^2})} - \rho I \frac{\partial^3 w}{\partial^2 t \partial x} \right], \\ Q_4^e &= - \left(EI \frac{\partial^2 w}{\partial x^2} \right).\end{aligned} \quad (8)$$

To perform time integration, the overall FE model to be solved at every instance t has a form of:

$$M\ddot{u} + Ku = F, \quad (9)$$

Where M and K are the overall mass and stiffness matrices, respectively and F is the generalized load vector. According to the Newmark's scheme, the following time approximation is applied:

$$\begin{aligned}u_{s+1} &= u_s + \Delta t \dot{u}_s + \frac{1}{2} \Delta t^2 (1 - \gamma) \ddot{u}_s + \gamma \ddot{u}_{s+1}, \\ \dot{u}_{s+1} &= \dot{u}_s + \Delta t (1 - \alpha) \ddot{u}_s + \alpha \ddot{u}_{s+1},\end{aligned} \quad (10)$$

The subscripts s and $s+1$ refer to the times $t = t_s$ and $t = t_{s+1}$. A stable solution is obtained using constant-average acceleration method, by setting $\alpha = \gamma = 1$ [21]. Simultaneous solution of (9) at the instance $s+1$ and (10) yields:

$$\begin{aligned}\left(K_{s+1} + \frac{2}{\Delta t^2 \gamma} M_{s+1} \right) u_{s+1} &= F_{s+1} + \\ M_{s+1} \left[\frac{2}{\Delta t^2 \gamma} u_s + \frac{2}{\Delta t \gamma} \dot{u}_s + \frac{1 - \gamma}{\gamma} \ddot{u}_s \right],\end{aligned} \quad (11)$$

Knowing u and its time derivatives at the time s and using equations (10) and (11), those at the time $s+1$ could be determined.

4 LOW-DIMENSIONAL MODEL DESCRIPTION

The main idea is to write the snapshots, u^k as linear combinations of the POD modes ϕ^k . Thus any snapshots may be written as:

$$\mathbf{u} = \sum_{k=1}^N \mathbf{a}^k \Phi^k, \quad (12)$$

Where, \mathbf{u} is the solution in the time domain and the number of snapshots N is assumed large and the POD coefficients \mathbf{a}^k must be determined as functions of time. These coefficients are computed using parts of the singular value decomposition. The above equation can be rewritten as:

$$\mathbf{u} = \sum_{k=1}^N w^k (V^T)^k \Phi^k, \quad (13)$$

Where, w^k is the singular values or orthogonal values and V^T is the orthogonal coordinate. Any member of the snapshots ensemble can be reconstructed using "Eq. (12)". It means that the 1st snapshot which is the initial condition of our problem may be written as:

$$(V^T)_0^k = \frac{\Phi^T \mathbf{u}_0}{w^k}. \quad (14)$$

If the dynamical system performs under a new initial condition, $\tilde{\mathbf{u}}$, the above equation can be used to estimate relative orthogonal coordinate as:

$$(\tilde{V}^T)^k = \frac{\Phi^T \tilde{\mathbf{u}}}{w^k}, \quad (15)$$

Therefore, the POD temporal modes can be recalculated by considering these new orthogonal coordinate as:

$$\mathbf{a} = w^k (\tilde{V}^T)^k, \tag{16}$$

And the resulting coefficients are used to reconstruct the response of the system due to the new initial condition using “Eq. (12)”.

5 HIGH ORDER SVD BASED LOW-DIMENSIONAL MODEL

HOSVD is an extension to tensors of standard SVD, which only applies to matrices. For the first time, the SVD method provides an ability to use the POD for non-square matrices. The SVD of an (M×N) matrix A can be shown by:

$$A = U \times W \times V^T \tag{17}$$

Where T stands for transpose, U and V are orthogonal matrices and W is a diagonal positive definite matrix with r nonzero arrays, called the singular values of A. the SVD of A is written as the following expression:

$$A_{ij} = \sum_{l=1}^N U_{il} W_l V_{jl}^T \tag{18}$$

If A consider as a high order tensor, A_{ijk} has to decompose to the matrices. Tensor decomposition is expressed by the following formulation:

$$A_{ijk} = \sum_{\eta\mu\zeta}^r \sigma_{\eta\mu\zeta} u_{i\eta} v_{j\mu} w_{k\zeta} \tag{19}$$

Figure 1 shows the tensor decomposition by HOSVD method. Where $\sigma_{\eta\mu\zeta}$ is the component of another third-order tensor, called as core tensor, and $u_{\eta i}, v_{\mu j}, w_{\zeta k}$ are the elements of three vectors that are known as the HOSVD modes, where $u_{\eta i}, v_{\mu j}, w_{\zeta k}$ are the components of some orthonormal systems.

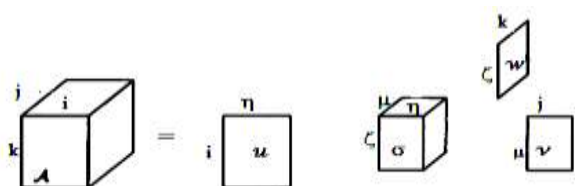


Fig. 1 Tensor decomposition by HOSVD.

The minimum value of r such that this decomposition is possible, is called the rank of the tensor A. To achieve the HOSVD modes first tensor A is decomposed to the symmetric matrices. On the following expression, any tensor can be decomposed to the symmetric matrices. The number of these symmetric matrices is referring to the number of variable parameters plus one.

$$B_{il}^1 = \sum_{j,k} A_{ijk} A_{ijk}$$

$$B_{jl}^2 = \sum_{i,k} A_{ijk} A_{ilk} \tag{20}$$

$$B_{kl}^3 = \sum_{i,j} A_{ijk} A_{ijl}$$

The HOSVD modes are given by result of an eigenvalues solution such as following:

$$\sum_{l=1}^{m_1} B_{il}^1 u_{i\eta} = (\alpha_{\eta})^2 u_{i\eta}, \quad \eta = 1, 2, \dots, r_1$$

$$\sum_{l=1}^{m_2} B_{jl}^2 v_{j\mu} = (\beta_{\mu})^2 v_{j\mu}, \quad \mu = 1, 2, \dots, r_2 \tag{21}$$

$$\sum_{l=1}^{m_3} B_{kl}^3 w_{k\zeta} = (\gamma_{\zeta})^2 w_{k\zeta}, \quad \zeta = 1, 2, \dots, r_3$$

Where ($r_i \leq m_i$) is the rank of the matrix B^i , the positive scalars $\alpha_{\eta}, \beta_{\mu}$ and γ_{ζ} will be referred to, as the high order singular values of the decomposition. Now after HOSVD modes calculated, the core tensor can be obtained:

$$\sigma_{\eta\mu\zeta} = \sum_{ijk} A_{ijk} u_{i\eta} v_{j\mu} w_{k\zeta} \tag{22}$$

And the field variables can be reconstructed by the equation (19).

6 ORDER REDUCTION CRITERION

Usually, when the number of modes is increased, the reconstruction is performed with better accuracy. It is required to use the optimal number of modes for data reconstruction. It is equivalent to capturing the highest level of energy and the least number of modes for model construction (“Fig. 1”). In this manner, a fraction number is defined for automatic selection of modes as follow:

$$\kappa = \frac{\sum_{i=1}^{N_r} \lambda_i}{\sum_{i=1}^{N_{total}} \lambda_i}, \quad (23)$$

Where, κ is about 99.9% and N_r is the optimum number of modes for reduced order model construction [3].

7 RESULTS

The results of this research will be presented in two parts. Firstly, the results obtained for an un-damped and damped linear cantilever beam under static loading are demonstrated using classic POD-ROM simulation framework. For validation of low-dimensional POD model, the outcome results, which are obtained POD-ROM, are compared with the related FEM data. Two ensembles with 500 members in different times with equal increments and in a specific time span were used as an input ensemble for damped and un-damped free vibration of a linear beam model. The second problem is about the development of a reduced order model based on the combination of the POD and HOSVD approaches. The results were obtained for the linear beam model in un-damped and damped forms and different values of beam thickness. Results of POD-HOSVD reduced order framework have been compared with the related FEM data. Two ensembles with 500 members in different times with equal time increments and in a specific time span and five thickness values were considered as an input data set for the damped and un-damped free vibration of a linear beam model.

7.1. Un-damped Vibration of Linear Beam Model

Un-damped free vibration of a linear cantilever beam from steel ($E = 200GPa$ and $\rho = 8000 kg/m^3$) with dimensions of $24 \times 1 \times 0.75$ (inch) was considered. The finite element model was created for the beam using 24 beam elements. First, deflections of the beam due to the three static loads, as to be shown in “Table 1”, were obtained.

Table 1 Loading Specification of Linear Beam Model

	Load, lbf	Position, in
L ₁	300	17
	200	18
	-260	24
L ₂	100	24
L ₃	-300	8

After the solution of eigenvalues problem, the POD modes (spatial modes) and their weights (temporal

modes), the effectiveness of each POD modes are calculated. By using approach presented in section 4.1., the number of modes to reconstruct data with the highest level of accuracy is calculated. In this problem, seven modes have been used to reconstruct field. Figure 2 shows the spatial distribution of four strongest POD modes (high energy level) of an ensemble in response to L₁. The relative energy distribution of the POD modes has been demonstrated in “Fig. 3”.

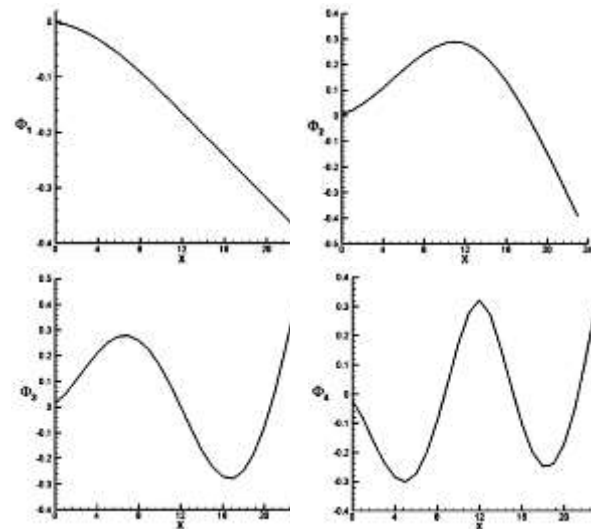


Fig. 2 Distribution of First Four Strongest POD Modes of the initial ensemble in response to loading L₁.

Figure 4 shows the distribution of estimated observations ensemble in response to L₂ and L₃. In “Figs. 5-6” the time variations of the tip displacement in response to L₂ and L₃ from reduced order model (compared to FEM data) are shown. It is clear from these figures that the low-dimensional model has relatively good agreements compared to the FEM data.

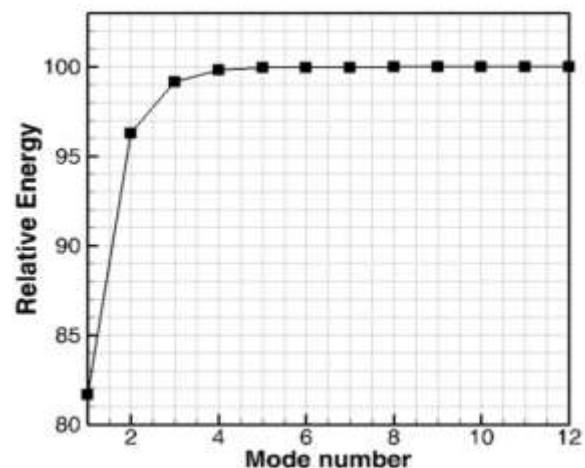


Fig. 3 Relative energy of POD modes, computed from the initial ensemble in response to loading L₁.

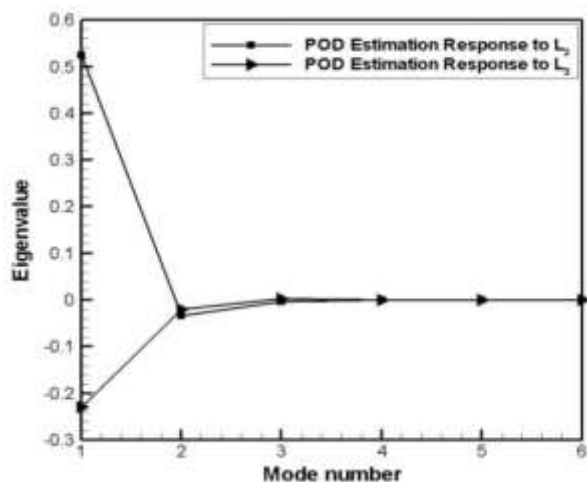


Fig. 4 Estimated eigenvalues distribution using low dimensional POD model in response to loading L_2 and L_3 .

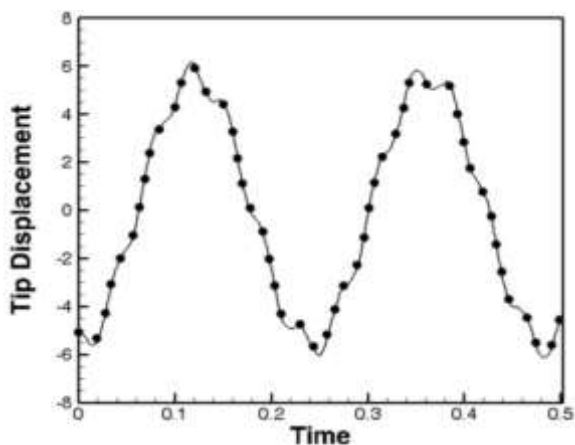


Fig. 5 Comparison between the prediction of tip displacement of the linear beam, Reduced order POD model (solid lines) and the FE model (points) in response to loading L_2 .

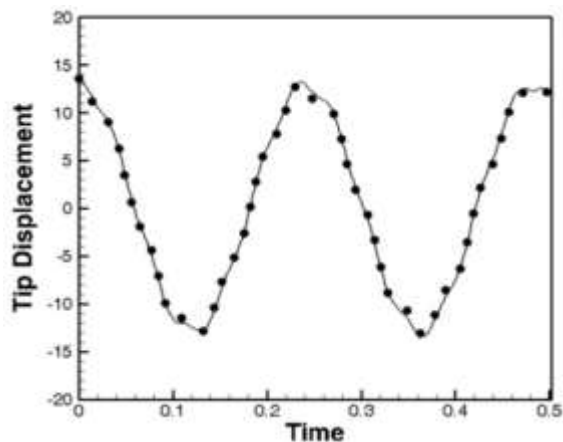


Fig. 6 Comparison between the prediction of tip displacement of the linear beam, Reduced order POD model (solid lines) and the FE model (points) in response to loading L_3 .

7.2. Damped Vibration of Linear Beam Model

Damped free vibration of a linear cantilever beam from steel ($E = 200GPa$ and $\rho = 8000 kg/m^3$) with dimensions of $24 \times 1 \times 0.75$ (inch) and with the damping coefficient $C = 35 N.s/m$ was considered. Also, in this case, the number of beam elements is 24 and the deflections of the beam were obtained under the conditions similar to “Table 1”. Figures 7 and 8 show the time variations of the tip displacement in response to L_2 and L_3 for the damped free vibration of the linear beam computed from the reduced order model (compared to FEM data). The outcome results show that the surrogate model can estimate relatively accurate results. In this case, due to the lack of damping, a limit cycle form of free vibration is seen.

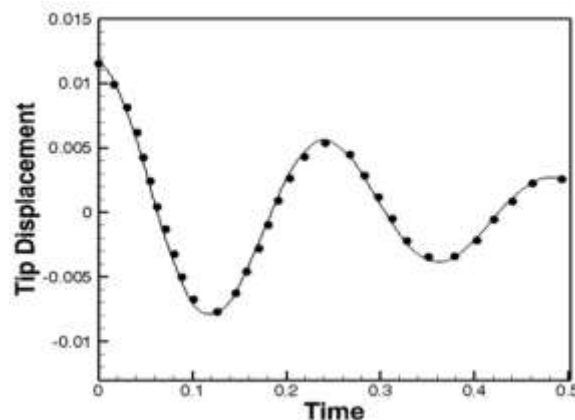


Fig. 7 Comparison between the prediction of tip displacement of the linear beam, Reduced order POD model (solid lines) and the FE model (points) in response to loading L_2 .

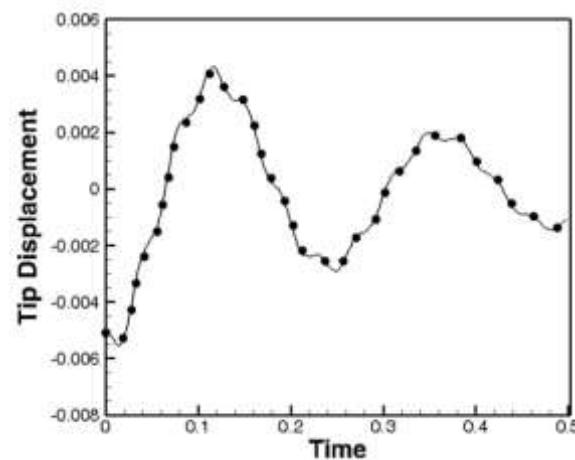


Fig. 8 Comparison between the prediction of tip displacement of the linear beam, Reduced order POD model (solid lines) and the FE model (points) in response to loading L_3 .

7.3. Damped Vibration of Non-linear Beam Model

The damped free vibration of a non-linear cantilever beam with a similar specification by linear beam test case was considered. For this test case, non-linear spring with the following forcing function is considered:

$$F_s(x) = ax + bx^2,$$

$$a = 1.75 \times 10^3 \frac{\text{N}}{\text{m}} \quad (23)$$

$$b = 1.629 \times 10^8 \frac{\text{N}}{\text{m}^3}$$

The finite element model was created for the beam using 24 beam elements. First, the deflections of the beam due to the three static loads, as reported in "Table 2", were obtained.

Table 2 Loading Specification of the Non-Linear Beam Model

	Load, lbf	Position, in
L ₁	300	17
	200	18
	-260	24
L ₂	100	24
L ₃	-300	8

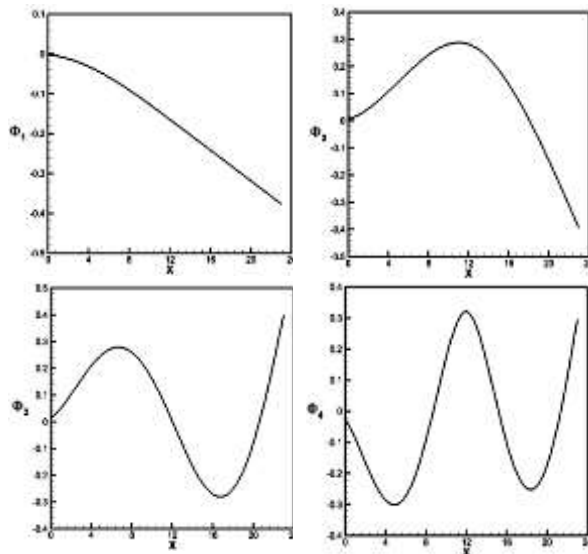


Fig. 9 Distribution of First Four Highest Energy Level POD Modes of the initial ensemble in response to loading L₁ for the Non-linear beam model.

The POD modes and their coefficients are calculated using singular value decomposition. For this problem 5 modes have been used to reconstruct the related reduced order model. Figure 9 shows spatial distribution of the four strongest POD modes of an ensemble in response to L₁. The relative energy distribution of the POD modes has been shown in the Fig. 10.

Figure 11 shows a comparison between the time variations of the tip displacement in response to L₂ from the reduced order model and FEM data. Also similar comparison between predictions of ROM and FEM data for time variations of tip displacement in response to L₃ has been shown in Fig. 12. It is clear from these figures that the reduced order model has relatively good agreements compared to the FEM data.

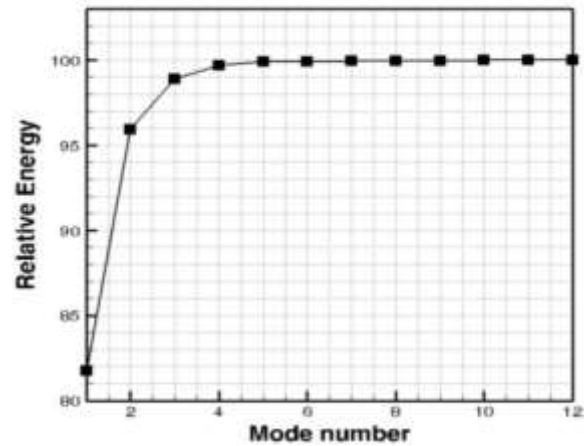


Fig. 10 Relative energy of POD modes, computed from the initial ensemble in response to loading L₁ for the Non-linear beam model.

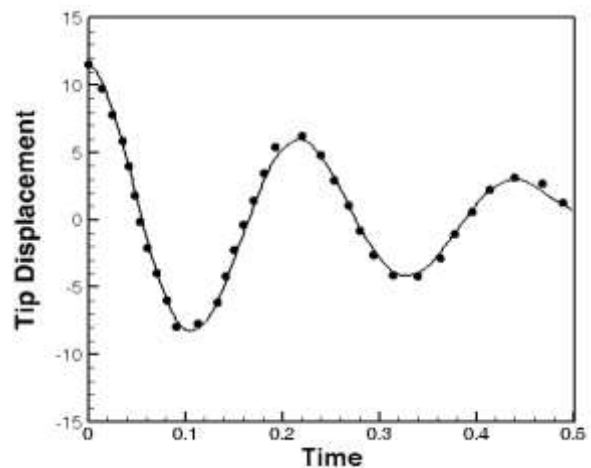


Fig. 11 Time variations of tip displacement of the non-linear beam, Reduced order model (solid lines) and the FE model (points) in response to loading L₂.

7.4. Un-damped Vibration Linear Beam Model under Variations of Thickness and Loading

In this section, the un-damped free vibration of a linear cantilever beam from steel with the similar specification of beam model described in section 7-1 and dimensions of 24×1×h (inch) was considered. The finite element model was applied for the beam using 24 elements. First, deflections of the beam due to the seven static loads from -300lb to 300lb, at the

end of the beam were obtained. Also, thickness (h) is changed between 0.25" to 1.5" for the present case and the damped vibration test case. After the solution of eigenvalues problem, the HOSVD modes (spatial modes) and their weights (temporal modes) and the related energy of each HOSVD modes are calculated. By using approach introduced previously, the number of modes for reconstruction of data with an appropriate level of accuracy is calculated.

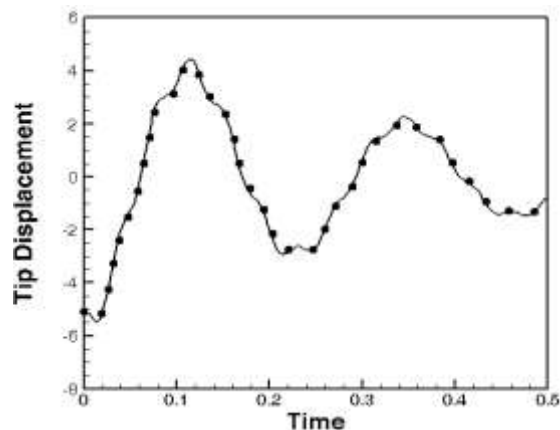


Fig. 12 Time variations of tip displacement of the non-linear beam, Reduced order model (solid lines) and the FE model (points) in response to loading L3.

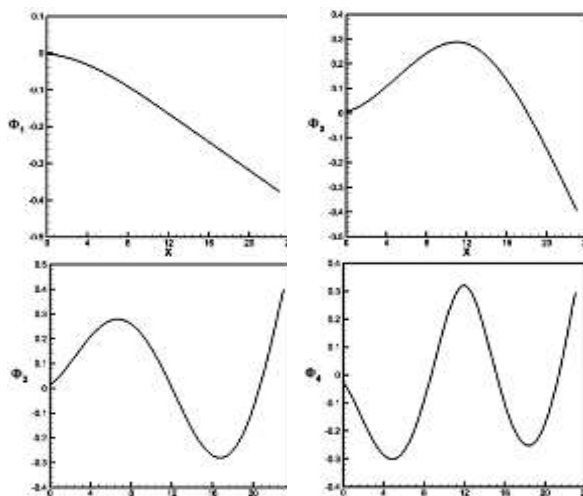


Fig. 13 Distribution of first four highest energy level POD Modes of the initial ensemble in response to loading L_1 for Non-linear beam model.

For this problem, five modes have been used to reconstruct the related field. Figure 13 shows the distribution of the four strongest HOSVD modes (high energy level) of an ensemble in response to different loads and beam thickness. The relative energy distribution of the HOSVD modes via diverse beam thickness has been demonstrated in “Fig. 14”. Figure 15 shows the distribution of relative energy of HOSVD modes via variation of tip loading.

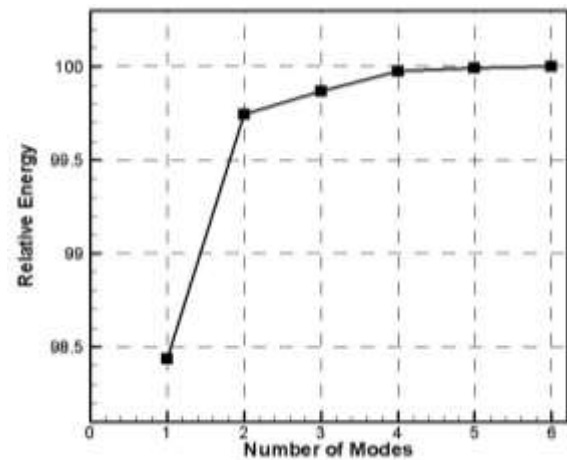


Fig. 14 Relative energy of HOSVD modes, computed via beam thickness variations.

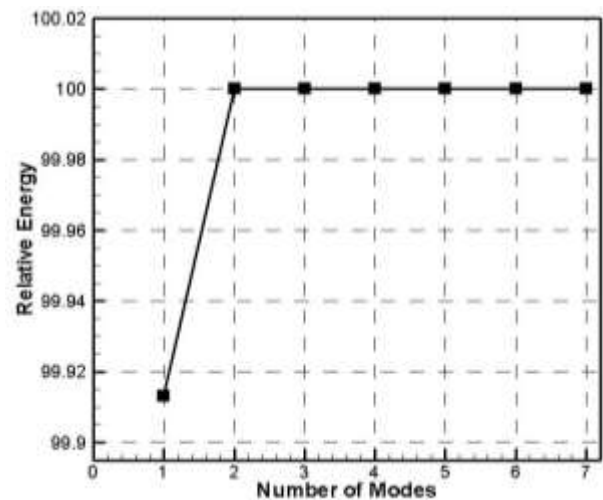


Fig. 15 Relative energy of HOSVD modes, computed via variations of loading.

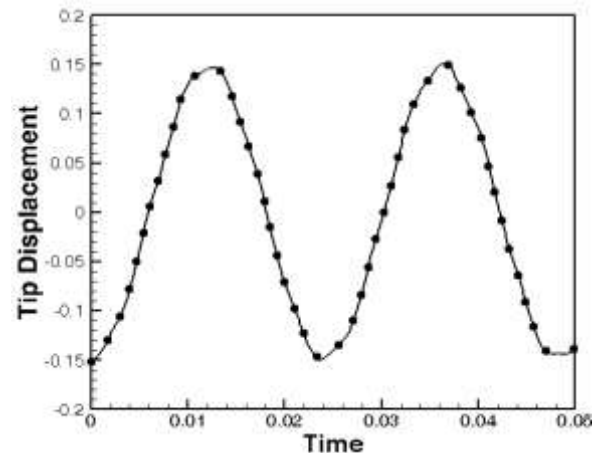


Fig. 16 Comparison between the prediction of tip displacement of the linear beam, Reduced order POD-HOSVD model (solid lines) and the FE model (points) in response to loading $L_2 = -150$ lb and $h=0.75$ in.

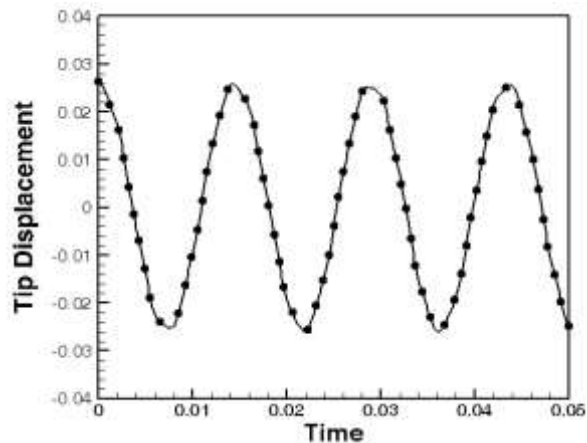


Fig. 17 Comparison between the prediction of tip displacement of the linear beam, Reduced order POD model (solid lines) and the FE model (points) in response to loading $L_3 = 200$ and $h=1.25$ in.

In “Figs. 16-17”, the time variations of the tip displacement in response to $L_2 = -150$ lb and $L_3 = 200$ lb loads, from reduced order model are shown. It is clear from the results of the reduced order model that this approach has good accuracy for predicting desired results compared to the FEM data.

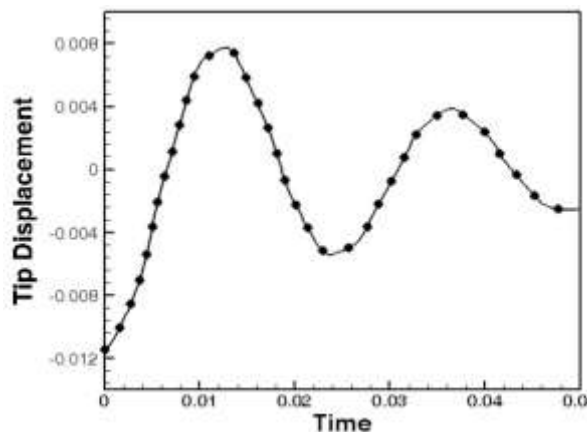


Fig. 18 Comparison between the prediction of tip displacement of the linear beam, Reduced order POD-HOSVD model (solid lines) and the FE model (points) in response to loading $L_2 = -120$ lb and $h=0.75$ in.

7.5. Damped Vibration of Linear Beam Model under Variations of Thickness and Loading

For the case of damped free vibration, a linear cantilever beam with steel material and dimensions of $24 \times 1 \times h$ inch was considered. The beam has specification similar to un-damped model but it contains a damping coefficient as $C = 35$ N.s/m. So, in this case, the number of beam elements is 24 and the deflections of the beam were obtained due to the static loading similar to the un-damped test case.

Figures 18 and 19 show the time variations of the tip displacement in response to $L_2 = -120$ lb, and $L_3 = 120$ lb, for damped free vibration of linear beam computed from reduced order model (compared to FEM data). It is very evident that the ROM based on POD-HOSVD has an excellent ability to predict accurate results even for a damped linear beam model.

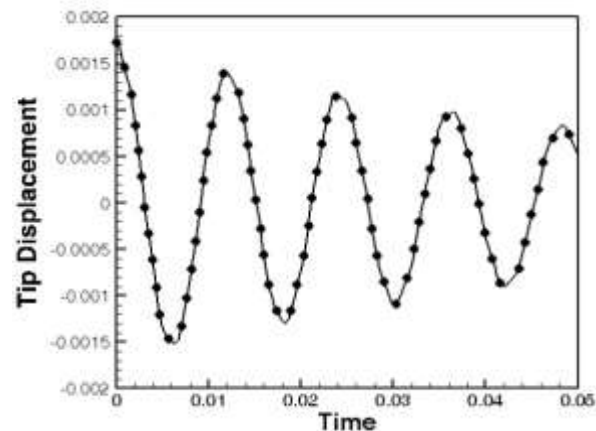


Fig. 19 Comparison between the prediction of tip displacement of the linear beam, Reduced order POD-HOSVD model (solid lines) and the FE model (points) in response to loading $L_3 = 120$ lb and $h=1.5$ in.

8 CONCLUSION

In recent years, great improvements have been made in advancing the applications and upgrading accuracy of proper orthogonal decomposition (POD)-based reduced order models (ROM). Some of these improvements for more accurate prediction of the dynamical systems are often discussed in the literature. It is clear that the POD is a robust method for estimation and simulation of the steady and unsteady problems, respectively. In this work, a POD snapshots method was used for calculation of the POD modes. Then, a low-dimensional approach for simulation of free vibration of an un-damped and damped linear beam has been used to compute the response of beam to the different initial data.

On the other hand, the HOSVD based POD method was used to build up a reduced order simulation framework. In particular, the work has focused on the ability of method for application in parametric spaces. Next, a low order model for simulation of free vibration of an un-damped and damped linear beam has been used to compute the response of beam to the different values of loading and beam's thickness. An order reduction manner was used to choose the minimum number of modes for reconstruction of the dynamical system and therefore it prepares a low-dimensional model for fast prediction of the problem and the current approach gives suitable results.

REFERENCES

- [1] Lucia, D. J., Beranb, P. S., and Silva, W. A., Reduced Order Modeling: New Approaches for Computational Physics, Progress in Aerospace Sciences, Vol. 40, 2004, pp. 51-117.
- [2] Holmes, P., Lumley, J. L., and Berkooz, G., Turbulence, Coherent Structures, Dynamical Systems and Symmetry, Cambridge Monographs on Mechanics, Cambridge University Press, 1996.
- [3] Taeibi-Rahni, M., Sabetghadam, F., and Moayyedi, M. K., Low-Dimensional Proper Orthogonal Decomposition Modeling as a Fast Approach of Aerodynamic Data Estimation, Journal of Aerospace Engineering, Vol. 23, Issue 1, 2010, pp. 44-54.
- [4] Sirovich, L., Kirby, M., Low-Dimensional Procedure for the Characterization of Human Faces, J. Optical Society of America, Vol. 4, No. 3, 1987, pp. 519-24.
- [5] Shinde S., Pandy M., Modelling Fluid Structure Interaction Using One-way Coupling and Proper Orthogonal Decomposition, Proceedings of the 11th International Conference on Engineering Sciences (AFM 2016), At Ancona, Italy, 2016.
- [6] Tissot, G., Cordier, L., Noack, B. R., Feedback Stabilization of an Oscillating Vertical Cylinder by Pod Reduced-Order Model, Journal of Physics: Conference Series, Vol. 574, 2015, pp. 012137.
- [7] Feeny, B. F., Kappagantu, R., On the Physical Interpretation of Proper Orthogonal Modes in Vibration, Journal of Sound and Vibration, Vol. 211, No. 4, 1998, pp. 607-616.
- [8] Han, S., Linking Proper Orthogonal Decomposition Modes and Normal Modes of the Structure, Proceedings of the 18th International Modal Analysis Conference (IMAC), 2000.
- [9] Kereschen, G., Golinval, J. C., Physical Interpretation of the Proper Orthogonal Modes using the Singular Value Decomposition, Journal of Sound and Vibration, Vol. 249, No. 5, 2002, pp. 849-865.
- [10] Han, S., Feeny, B., Application of Proper Orthogonal Decomposition to Structural Vibration Analysis, Mechanical Systems and Signal Processing, Vol. 17, No. 5, 2003, pp. 989-1001.
- [11] Amabili, M., Sarkar, A., and Païdoussis, M. P., Reduced-Order Models for Nonlinear Vibrations of Cylindrical Shells Via the Proper Orthogonal Decomposition Method, Journal of Fluids and Structures, Vol. 18, No. 2, 2003, pp. 227-250.
- [12] Lieu, T., Farhat, C., Adaptation of POD-Based Aeroelastic ROMs for Varying Mach Number and Angle of Attack: Application to a Complete F-16 Configuration, AIAA Paper 2005-7666, U.S. Air force T&E Days, Tennessee, 2005.
- [13] Gonçalves, P. B., Prado, Z. J. G. N. D., Low-Dimensional Galerkin Models for Nonlinear Vibration and Instability Analysis of Cylindrical Shells, Nonlinear Dynamics, Vol. 41, No. 1, 2005, pp. 129-145.
- [14] Georgiou, I., Advanced Proper Orthogonal Decomposition Tools: Using Reduced Order Models to Identify Normal Modes of Vibration and Slow Invariant Manifolds in the Dynamics of Planar Nonlinear Rods, Nonlinear Dynamics, Vol. 41, No. 1, 2005, pp. 69-110.
- [15] Allison, T. C., System Identification via the Proper Orthogonal Decomposition, PhD Dissertation, Dep't Mechanical Engineering, Virginia Polytechnic Institute and State University, 2007.
- [16] Gonçalves, P. B., Silva, F. M. A., Del Prado, Z. J. G. N., Low-dimensional Models for the Nonlinear Vibration Analysis of Cylindrical Shells Based on a Perturbation Procedure and Proper Orthogonal Decomposition, Journal of Sound and Vibration, Vol. 315, No. 3, 2008, pp. 641-663.
- [17] Gonçalves, P. B., Silva, F. M. A., Del Prado, Z. J. G. N., Reduced Order Models for the Nonlinear Dynamic Analysis of Shells, Procedia IUTAM, Vol. 19, 2016, pp. 118-125.
- [18] Speet, J., Parametric Reduced Order Modeling of Structural Models by Manifold Interpolation Techniques, M.Sc. Thesis, Department of Mechanical Engineering at Delft University of Technology, 2017.
- [19] Ilbeigi, S., A New Framework for Model Reduction of Complex Nonlinear Dynamical Systems, PhD Dissertation, Department of Mechanical Engineering at University of Rhode Island, 2017.
- [20] Guo, M., Hesthaven, J. S., Reduced Order Modeling for Nonlinear Structural AnalysisU Gaussian Process Regression, Computer Methods in Applied Mechanics and Engineering, Vol. 341, 2018, pp. 807-826.
- [21] Reddy, J. N., An Introduction to Finite Element Method, 3rd Edition, McGraw Hill, 2006.